by Noyes[8] in bromate oscillators. Development of even this level of mechanistic detail will surely involve the introduction of a number of intermediate species such as HOI and HIO_2 and probably such binuclear intermediates as $H_2I_2O_3$ and $ICIO_2$, for which there is already support in studies of the component processes.[21,24,25]

Acknowledgment. We thank Professor Kenneth Kustin for helpful discussions and a critical reading of the manuscript. This work was supported by Grant CHE7905911 from the National Science Foundation.

Registry No. ClO_2^-, 14988-27-7; I^-, 20461-54-5; IO_3^-, 15454-31-6; $Cr_2O_7^{2-}$, 13907-47-6; MnO_4^-, 14333-13-2; BrO_3^-, 15541-45-4; I_2, 7553-56-2; $Fe(CN)_6^{4-}$, 13408-63-4; SO_3^{2-}, 14265-45-3; $S_2O_3^{2-}$, 14383-50-7; H_3AsO_3, 36465-76-6.

Bistability in the Oxidation of Iron(II) by Nitric Acid[1]

Miklós Orbán[2] and Irving R. Epstein*

Contribution from the Department of Chemistry, Brandeis University, Waltham, Massachusetts 02254. *Received March 30, 1982*

Abstract: The autocatalytic reaction between ferrous ion and nitric acid has been studied at 25 °C in a continuous flow stirred tank reactor. The system exhibits bistability as a function of flow rate for a wide range of Fe(II) and HNO_3 input fluxes. The results obtained are in good agreement with a seven-step mechanism proposed earlier to account for the batch ferrous–nitric acid clock reaction. The possibility of constructing a chemical oscillator based on this system is discussed briefly.

Autocatalytic reactions in flow systems are of considerable interest because they may give rise to bistability or multistability, the existence of two or more *different* stable steady states of a system subject to the *same* set of imposed constraints. Which of the two states is attained in any particular experiment then depends only upon the past history of the system. This rather surprising behavior, which is possible only in an open chemical system, has been shown to be intimately related[3] to another fascinating phenomenon, chemical oscillation.

In the past year, a number of new bistable[4,5] and even tristable[1] systems have been developed starting from reactions previously known to be autocatalytic. Some of these systems have been further modified so as to produce oscillation.[4b,6] However, in contrast to the cerium bromate–bromide system studied earlier by Geiseler and Bar-Eli,[7] the autocatalytic reactions involved in these new systems have not been well enough understood mechanistically to allow a detailed comparison of calculated and experimental results.

In this paper, we present an experimental study of bistability in the autocatalytic oxidation of iron(II) by nitric acid in a stirred tank reactor (CSTR). An earlier investigation of this system under batch conditions combined with other work on related systems yielded a seven-step mechanism which gave excellent agreement with the observed behavior.[8] Here we use this mechanism to simulate the new flow experiments. Comparison of the results provides both a more stringent test of the mechanism and improved values for some of the free parameters in that scheme.

Table I. Reaction Scheme and Rate Expression Employed in Computer Simulations

no.	reaction and velocity	ref
P1	$Fe^{2+} + NO_3^- + 2H^+ = Fe^{3+} + NO_2 + H_2O$ $v_1 = 1.0 \times 10^{-7}\ M^{-1}\ s^{-1}[Fe^{2+}][NO_3^-]$ $v_{-1} = 1.4 \times 10^{-5}\ M\ s^{-1}[Fe^{3+}][NO_2]/[H^+]^2$	this work, 9, 10
P2	$Fe^{2+} + NO_2 + H^+ = Fe^{3+} + HNO_2$ $v_2 = 3.1 \times 10^4\ M^{-1}\ s^{-1}[Fe^{2+}][NO_2]$ $v_{-2} = 6.5 \times 10^{-4}\ s^{-1}[Fe^{3+}][HNO_2][H^+]$	9–11
P3	$Fe^{2+} + HNO_2 + H^+ = Fe^{3+} + NO + H_2O$ $v_3 = (7.8 \times 10^{-3}\ M^{-1}\ s^{-1} + 2.3 \times 10^{-1}\ M^{-2}\ s^{-1}[H^+] + 7.6 \times 10^{-3}\ M^{-1}\ s^{-1}[HNO_2]/[NO])[Fe^{2+}][HNO_2]$ $v_{-3} = (5.6 \times 10^{-4}\ s^{-1}[NO]/[H^+] + 1.6 \times 10^{-2}\ M^{-1}\ s^{-1}[NO] + 5.4 \times 10^{-4}\ s^{-1}[HNO_2]/[H^+])[Fe^{3+}]$	10–12
P4	$Fe^{2+} + NO = FeNO^{2+}$ $v_4 = 6.2 \times 10^5\ M^{-1}\ s^{-1}[Fe^{2+}][NO]$ $v_{-4} = 1.4 \times 10^3\ s^{-1}[FeNO^{2+}]$	13
P5	$2NO_2 + H_2O = HNO_2 + NO_3^- + H^+$ $v_5 = 1.0 \times 10^6\ M^{-1}\ s^{-1}[NO_2]^2$ $v_{-5} = 1.5 \times 10^{-2}\ M^{-2}\ s^{-1}[HNO_2][NO_3^-][H^+]$	9, 10
P6	$2HNO_2 = NO + NO_2 + H_2O$ $v_6 = 5.8\ M^{-1}\ s^{-1}[HNO_2]^2$ $v_{-6} = 2.0 \times 10^7\ M^{-1}\ s^{-1}[NO][NO_2]$	9, 10, 14
P7	$NO + NO_3^- + H^+ = NO_2 + HNO_2$ $v_7 = 5.0 \times 10^{-3}\ M^{-3}\ s^{-1}[NO_3^-][NO][H^+]^2$ $v_{-7} = 9.3\ M^{-2}\ s^{-1}[HNO_2][NO_2][H^+]$	this work, 9, 10

Experimental Section

Materials. High-purity $FeSO_4 \cdot 7H_2O$, HNO_3, and NO were available commercially. Nitric acid solutions were purged with N_2 for 1 h or more to remove dissolved gases. Ferrous solutions were freshly made for each experiment and were also purged with nitrogen. The NO used in the determination of the $FeNO^{2+}$ extinction coefficient was first passed through a 30-cm column of NaOH to remove any NO_2 present.

Reactor. The CSTR used has been described previously.[4a] However, it was found that the presence of oxygen and/or nitrogen oxides in the space between the liquid surface and the reactor cap impaired the reproducibility of the experiments. The reactor was then modified to eliminate this space so that the liquid completely filled the reactor volume of 28.6 cm^3. The reactor was thermostated at 25.0 ± 0.1 °C.

(1) Part 12 in the series Systematic Design of Chemical Oscillators. Part 11: Orbán, M.; Dateo, C.; De Kepper, P.; Epstein, I. R. *J. Am. Chem. Soc.*, preceding paper.

(2) Institute of Inorganic and Analytical Chemistry, L. Eötvös University, H-1443 Budapest, Hungary.

(3) Boissonade, J.; De Kepper, P. *J. Phys. Chem.* **1980**, *84*, 501–506.

(4) (a) De Kepper, P.; Epstein, I. R.; Kustin, K. *J. Am. Chem. Soc.* **1981**, *103*, 6121–6127. (b) Dateo, C. E.; Orbán, M.; De Kepper, P.; Epstein, I. R. *Ibid.* **1982**, *104*, 504–509. (c) Epstein, I. R.; Dateo, C. E.; De Kepper, P.; Kustin, K.; Orbán, M. In "Non-Linear Phenomena in Chemical Dynamics"; Vidal, C., Pacault, A., Eds.; Springer: New York, 1981; Vol. 12, pp 188–191.

(5) (a) Papsin, G. A.; Hanna, A.; Showalter, K. *J. Phys. Chem.* **1981**, *85*, 2575–2582. (b) Reckley, J. S.; Showalter, K. *J. Am. Chem. Soc.* **1981**, *103*, 7012–7013.

(6) (a) De Kepper, P.; Epstein, I. R.; Kustin, K. *J. Am. Chem. Soc.* **1981**, *103*, 2133–2134. (b) Orbán, M.; De Kepper, P.; Epstein, I. R.; Kustin, K. *Nature (London)*, **1981**, *292*, 816–818. (c) De Kepper, P.; Epstein, I. R.; Kustin, K.; Orbán, M. *J. Phys. Chem.* **1982**, *86*, 170–171. (d) Orbán, M.; De Kepper, P.; Epstein, I. R. *Ibid.* **1982**, *86*, 431–433.

(7) Geiseler, W.; Bar-Eli, K. *J. Phys. Chem.* **1981**, *85*, 908–914.

(8) Epstein, I. R.; Kustin, K.; Warshaw, L. J. *J. Am. Chem. Soc.* **1980**, *102*, 3751–3758.

0002-7863/82/1504-5918$01.25/0 © 1982 American Chemical Society

Spectrophotometric Analysis. Measurements were made of the absorbance of the solution at 450 nm, the wavelength of maximum absorbance of the $FeNO^{2+}$ complex. The extinction coefficient, for which a lower limit of 80 is given in ref 8, was carefully redetermined as follows. The CSTR was filled with Fe^{2+} solution. The flow was stopped and the solution was purged with N_2 for 20 min. Nitric oxide was then introduced through a capillary tube at a constant rate and the optical density was monitored until it reached saturation (3–5 min). The complex is stable if the partial pressure of NO is maintained at ~1 atm and no O_2 is present, but it decomposes rapidly in the presence of oxygen. Experiments in 1.25 N H_2SO_4, with $[Fe^{2+}]$ ranging from 3×10^{-4} to 1×10^{-3} M give $\epsilon_{450} = 219 \pm 10$. Approximately the same value was obtained when the 1.25 N H_2SO_4 was replaced by 1.5 N H_2SO_4 or 1.5 M $NaNO_3$ or a pH 2 Na_2SO_4–H_2SO_4 buffer solution.

Mechanism and Kinetics

The reactions and rate expressions used to describe the Fe(II)–HNO_3 system[8] are summarized in Table I. The thermodynamic data relevant to these reactions are given in ref 8, where a discussion of the elementary steps which comprise reactions P1, P2, P3, and P7 may also be found. The rate constants for reactions P2–P6 were obtained from a variety of kinetics studies and equilibrium data. The quantities k_1 and k_7 were not measured directly, but were estimated by optimizing the agreement between the calculated and experimental batch results.[8]

In this work we have utilized the recent determination of Lee and Schwartz[9] of the solubility of NO_2 and of its rate of hydrolysis, reaction P5. The experiments presented here were carried out at considerably lower ionic strength than employed in ref 8, and several measurements failed to reveal any significant dependence of the bistability behavior on ionic strength. We have therefore not introduced any activity coefficient corrections, though certainly activities of some species must differ from unity. In the earlier study,[8] nitric acid solutions were assumed to contain HNO_2 as an impurity, according to the equation $[HNO_2]_0 = C_0[H^+]_0 - [NO_3^-]_0$. In view of the greater care exercised here to purge the solutions prior to use, the value of C_0 was lowered from 2×10^{-6} to 1×10^{-9} M^{-1}. This parameter has negligible effect in simulations of the flow experiments, but does influence and was estimated from the results of the batch calculations reported below.

Simulations of the flow experiments are considerably more sensitive to the value of k_1 than were the batch simulations. Both types of simulation are markedly affected by changes in k_7. The values given for these parameters in Table I represent improved estimates which give the best agreement between calculated and experimental results for both batch and flow conditions.

Results

Bistability. A series of experiments and calculations were carried out to determine whether and over what range of constraints the Fe(II)–HNO_3 system exhibits bistability. In each run, the input concentrations $[Fe(II)]_0$ and $[HNO_3]_0$, which the species would reach in the reactor as a result of the flow in the absence of chemical reaction, were fixed, and the flow rate (reciprocal of the residence time) k_0 was increased stepwise from zero to our maximum attainable value of 12.4×10^{-3} s^{-1} and then decreased back to zero. The absorbance of the solution at 450 nm and the potential of a Pt electrode (vs. $Hg|Hg_2SO_4$ reference electrode) were recorded. After each change in the flow rate, the system was allowed to attain steady-state values of both absorbance A and potential V.

If the system possesses a unique steady state, then the steady values of A and V observed at a given k_0 should be independent of whether the measurement is made during the increasing or

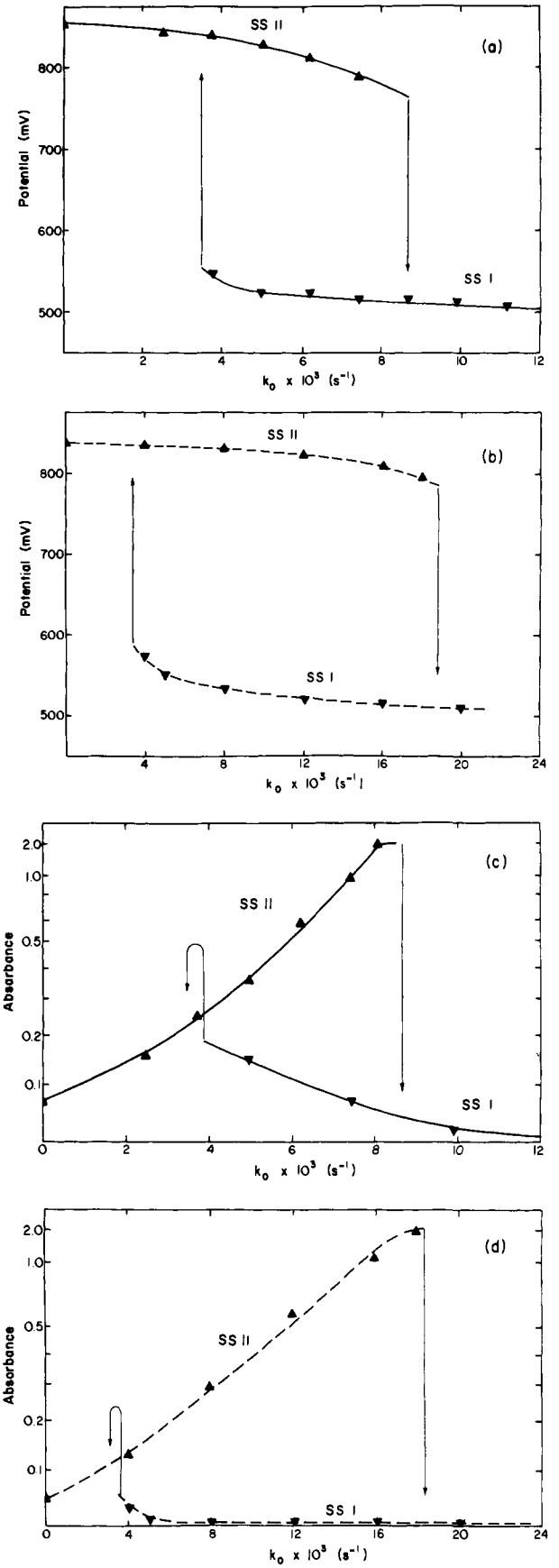

Figure 1. Steady-state potential of a platinum redox electrode (V) and absorbance at 450 nm (A) as functions of flow rate k_0 in a CSTR with $[Fe^{2+}]_0 = 0.075$ M, $[HNO_3]_0 = 1.25$ M: (a) observed V vs. k_0, (b) calculated V vs. k_0, (c) observed A vs. k_0, (d) calculated A vs. k_0. Vertical arrows indicate transitions between different branches of states: (SS I) high $[Fe^{2+}]$, low $[Fe(NO)^{2+}]$ (low potential state); (SS II) low $[Fe^{2+}]$, high $[Fe(NO)^{2+}]$ (high potential state).

(9) Lee, Y.-N.; Schwartz, S. B. *J. Phys. Chem.* **1981**, *85*, 840–848.
(10) Latimer, W. M. "Oxidation Potentials", 2nd ed.; Prentice-Hall: Englewood Cliffs, N.J., 1952.
(11) Abel, E.; Schmid, H.; Pollak, F. *Monatsh. Chem.* **1936**, *69*, 125–143.
(12) Winkler, L. W. *Ber.* **1901**, *34*, 1408–1422.
(13) Kustin, K.; Taub, I. A.; Weinstock, E. *Inorg. Chem.* **1966**, *5*, 1079–1080.
(14) Bunton, C. A.; Llewellyn, D. R.; Stedman, G. In "Recent Aspects of the Inorganic Chemistry of Nitrogen"; *Chem. Soc. Spec. Publ.* **1957**, *No. 10*, 113–122.

Table II. Calculated Steady-State Concentration (M) with $[Fe^{2+}]_0 = 0.075$ M, $[HNO_3]_0 = 1.50$ M, $k_0 = 8 \times 10^{-3}$ s^{-1}

	$[Fe^{2+}]$	$[Fe^{3+}]$	$[FeNO^{2+}]$	$[NO_3^-]$	$[NO_2]$	$[HNO_2]$	$[NO]$	$[H^+]$
low pot. state	7.5×10^{-2}	2.3×10^{-4}	4.9×10^{-5}	1.50	4.2×10^{-10}	1.4×10^{-5}	1.5×10^{-6}	1.50
high pot. state	3.3×10^{-3}	7.2×10^{-2}	2.0×10^{-4}	1.46	3.1×10^{-6}	3.6×10^{-2}	1.3×10^{-4}	1.39
Δ^a	−0.0717	0.0717		−0.037		0.036		−0.110
$\Delta/(0.036)$	−1.99	1.99		−1.03		1.00		−3.06

[a] Change from input flow, i.e., net production or consumption of major species in the reactor.

decreasing flow segment of the experiment. A bistable system, in contrast, will exhibit hysteresis, i.e., a range of k_0 over which two different sets of steady-state A and V values are observed for the increasing and decreasing flow segments. In Figure 1a,c we illustrate the hysteresis behavior for a typical experiment showing bistability.

The experimental measurements were simulated by integrating the rate equations of Table I with appropriate terms added to account for the input fluxes of Fe(II) and HNO_3 ($k_0[HNO_3]_0$ and $k_0[Fe^{2+}]_0$, respectively) and for the output fluxes of all species ($-k_0[X]$ for each species X). The calculations were performed using Hindmarsh's version[15] of the Gear method,[16] and sample results are shown in Figure 1b,d.

The potential measured by the platinum electrode is certainly a mixed potential, involving both the [Fe(II)]/[Fe(III)] ratio and the oxidation states of the nitrogen species. The calculated potentials in Figure 1b were obtained by applying the Nernst equation to the half-reaction

$$2H^+ + NO_3^- + e^- \rightarrow NO_2 + H_2O \quad (1)$$

to yield

$$E(\text{volts}) = E^\circ + 0.059 \log ([NO_2]/[H^+]^2[NO_3^-]) \quad (2)$$

where the value of E°, chosen empirically as 1.175 V, includes both the standard half-cell potential of 0.800 V and the effect of the $Hg|Hg_2SO_4|K_2SO_4$ reference electrode. Potential values calculated using the Fe^{2+}/Fe^{3+} half-reaction are nearly identical.

The qualitative agreement between the calculated and experimental absorbances and potentials is seen to be excellent. The only major discrepancy is that the transition at high flow rate is calculated to occur at a k_0 nearly twice that observed experimentally. The fact that when A is very low the calculated absorbances lie well below the experimental values may be accounted for by the contribution of an additional absorbing species such as NO_2 to the observed optical density. In both the experiments and the simulations, the difference in potential between the two branches of steady states is about 330 mV indepdendent of $[Fe(II)]_0$ and $[HNO_3]_0$, while the steady-state absorbances vary significantly with the input concentrations.

If a change in k_0 results in the system remaining on the same branch of steady states, then relaxation to the new steady state typically requires a few minutes. However, if increasing or decreasing k_0 produces a transition to the other branch of states as shown by the vertical arrows in Figure 1, then relaxation is quite slow, and the system may require an hour or more to reach the new state. This behavior, which is found both in our experiments and the numerical simulations, is related to the phenomenon of critical slowing down.[17] The calculations also predict the sizable overshoots in V and A which occur at the transitions between branches.

Two series of experiments were carried out: one to investigate the dependence of the bistable region on $[Fe(II)]_0$, the other to test the $[HNO_3]_0$ dependence. In the first series $[HNO_3]_0$ was fixed at 1.25 M, and the search for bistability with varying k_0 was performed at six different $[Fe(II)]_0$ values ranging from 0.025 to 0.15 M. The second series consisted of runs conducted at five different $[HNO_3]_0$ ranging from 0.9 to 1.75 M with $[Fe(II)]_0$ fixed at 0.075 M. The results, which constitute a portion of the system phase diagram,[1] are summarized in Figure 2.

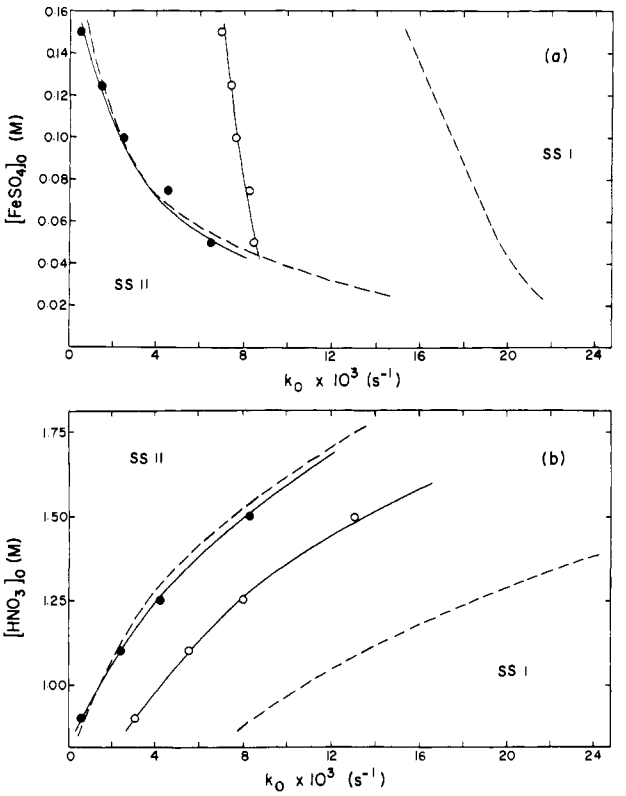

Figure 2. Phase diagrams (a) in the $[Fe^{2+}]_0$–k_0 plane with $[HNO_3]_0 = 1.25$ M and (b) in the $[HNO_3]_0$–k_0 plane with $[Fe^{2+}]_0 = 0.075$ M. Symbols: (●) experimentally observed transitions from SS I to SS II, (○) experimentally observed transitions from SS II to SS I. Area between the solid lines is the measured region of bistability. Area between the dashed lines is the calculated region of bistability.

We see that the qualitative agreement between the calculated and observed regions of bistability is excellent. The predicted lower k_0 boundary of the bistable region is in almost quantitative agreement with experiment for both the $[Fe(II)]_0$ and the $[HNO_3]_0$ variations. Although the k_0 values predicted for the upper boundary of the bistable region are too high by a factor of about 2 in both series of runs, the shape of the region (i.e., the variation of the critical k_0 with $[Fe(II)]_0$ or $[HNO_3]_0$) is given correctly by the simulations. No further adjustment of the free parameters k_1 and k_7 was found to remove the discrepancy between the observed and calculated upper boundaries.

In Table II, we give the steady-state values calculated for all chemical species in our model for both steady states at a typical point in the bistable region. Examination of the steady-state concentrations of the major species in the high potential state reveals that the changes from the input concentrations correspond almost exactly to the stoichiometry of the net process

$$2Fe^{2+} + NO_3^- + 3H^+ = 2Fe^{3+} + HNO_2 + H_2O$$

This state, which is the only stable one as $k_0 \rightarrow 0$, thus lies on the thermodynamic or equilibrium branch. The low potential state,

(15) Hindmarsh, A. C. "GEAR: Ordinary Differential Equation System Solver"; Technical Report No. U010-3001, Rev. 2; Lawrence Livermore Laboratory: 1972.

(16) Gear, C. W. "Numerical Initial Value Problems in Ordinary Differential Equations"; Prentice Hall: Englewood Cliffs, N.J., 1971; Chapter 11.

(17) (a) Schlögl, F. *Z. Phys.* **1971**, *248*, 446–458. (b) Heinrichs, M.; Schneider, F. W. *J. Phys. Chem.* **1981**, *85*, 2112–2116.

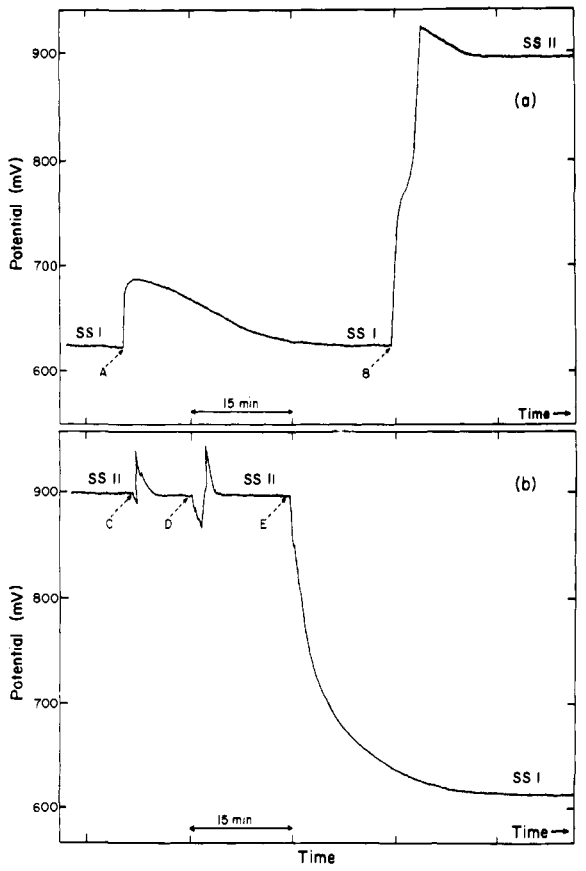

Figure 3. Perturbation experiments with $[Fe^{2+}]_0 = 0.125$ M, $[HNO_3]_0 = 1.25$ M, $k_0 = 4.9 \times 10^{-3}$ s^{-1}: (a) transition from SS I to SS II by nitrite perturbation; (b) transition from SS II to SS I by sulfite perturbation. At the lettered points the following concentration perturbations were made by a single rapid addition of the appropriate reagent: (A) $\Delta[NO_2^-] = 1.8 \times 10^{-2}$ M, (B) $\Delta[NO_2^-] = 7.2 \times 10^{-2}$ M, (C) $\Delta[SO_3^{2-}] = 1.0 \times 10^{-2}$ M, (D) $\Delta[SO_3^{2-}] = 2.5 \times 10^{-2}$ M, (E) $\Delta[SO_3^{2-}] = 3.6 \times 10^{-2}$ M.

which corresponds to the flow branch stable at high k_0, is seen to have steady-state concentrations nearly unchanged from those of the input flows.

Perturbation Experiments. A characteristic feature of any bistable system is its response to perturbation. Within the bistable region, a perturbation of either steady state results in relaxation back to that state if the perturbation is below a critical value, but a supercritical perturbation will induce a transition to the other steady state. The relaxation and/or the transition may be accompanied by transient overshoot and undershoot behavior.

Several experiments were carried out in which the Fe^{2+}–HNO_3 system at fixed values of k_0, $[Fe^{2+}]_0$, and $[HNO_3]_0$ was perturbed by single injections of nitrite or sulfite. As we see in Figure 3, sufficiently high nitrite perturbations induce a transition from the low to the high potential state with no overshoot for the subcritical and a single overshoot for the supercritical perturbation. Sulfite additions to the high potential state produce either return to the initial state with over- and undershoots or, if sufficiently large, smooth transition to the low potential state.

Simulations of the nitrite perturbation under the conditions of Figure 3 qualitatively predict the observed behavior, though the calculated critical nitrite perturbation is too small by about a factor of 4. It is more difficult to simulate the sulfite perturbation experiments, since it is not obvious which species reacts with the sulfite. However, we note that the critical sulfite concentration is roughly half the value we calculate for $[HNO_2]$ in the high-potential steady state and about one-fourth the ferric ion concentration in that state. Apparently, sulfite reacts rapidly with nitrous acid and/or ferric ion.

$$HSO_3^- + 2HNO_2 \rightarrow SO_4^{2-} + 2NO + H_2O + H^+ \quad (3)$$

$$HSO_3^- + 2Fe^{3+} + H_2O \rightarrow SO_4^{2-} + 2Fe^{2+} + 3\,H^+ \quad (4)$$

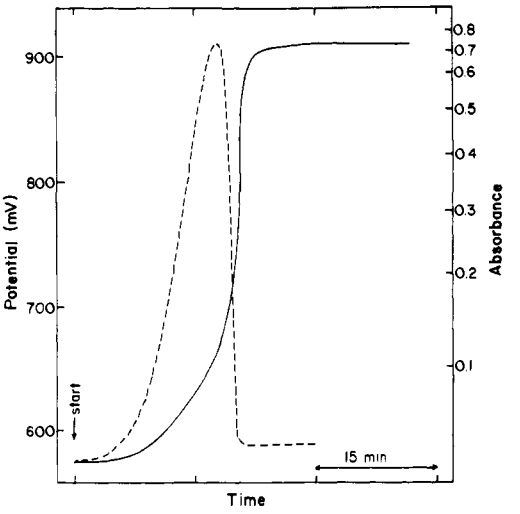

Figure 4. Potential of Pt electrode (—) and absorbance at 450 nm (---) for a batch experiment ($k_0 = 0$) with $[Fe^{2+}]_0 = 0.025$ M, $[HNO_3]_0 = 1.25$ M.

Table III. Experimental and Calculated Batch Reaction Times[a]

$[Fe^{2+}]_0$ (M)	$[HNO_3]_0$ (M)	t_{exptl} (min)	t_{calcd} (min)
0.025	1.25	16	10
0.050	1.25	24	16
0.075	1.25	45	27
0.100	1.25	50	52
0.125	1.25	75	88
0.150	1.25	102	136
0.075	0.90	90	96
0.075	1.10	65	43
0.075	1.25	45	27
0.075	1.50	20	15
0.075	1.75	6	9

[a] Time between filling of reactor and peak in $FeNO^{2+}$ absorbance.

No rate constants for these reactions were found in the literature, and our experimental attempts to estimate the relative rates of reactions 3 and 4 revealed only that they are both too rapid for conventional mixing techniques. For the conditions of Figure 3, the calculated critical $[NO_2^-]$ and $[SO_3^{2-}]$ perturbations are 1×10^{-2} and 3×10^{-2} M, respectively. While the simulation qualitatively predicts the observed over- and undershoots, it significantly underestimates their magnitude.

Batch Experiments. In a closed system, the ferrous–nitric acid reaction is a clock reaction, exhibiting a sharp absorbance peak at a time which depends strongly upon the reactant concentrations. The mechanism we employ for this system was established largely by testing its predictions of these batch reaction times.[8] Since we have modified several of the parameters used in the earlier study,[8] one may ask whether the model still gives accurate predictions of batch as well as flow experiments.

For each set of initial concentrations used in our flow studies, a batch experiment was done in which the reactor was filled, the pump turned off, and the absorbance followed to determine the time of the $[FeNO^{2+}]$ maximum. Results of a typical batch experiment are shown in Figure 4. The results and the corresponding times obtained in the simulations are given in Table III. The agreement is generally good, certainly as good as that obtained with the earlier parameter values.[8]

Discussion

The results presented above show that the mechanism developed to explain the autocatalytic clock reaction in batch Fe^{2+}–HNO_3 systems, with slight adjustments in the two free parameters k_1 and k_7, gives very good qualitative agreement with the more extensive data obtained in the flow experiments. A rapid mixing study of the reaction of a ferrous phenanthroline complex with nitrous acid[18] also showed good agreement between the predictions

of this model and the experimental data. We may thus have some confidence in the basic structure of the mechanism, though better quantitative agreement between experiment and simulation would be highly desirable. Such improvement might be obtained by a more accurate treatment of ionic strength effects and/or by inclusion of N_2O_3, N_2O_4, NO_2^-, and NO^+ as independent species in addition to NO, NO_2, and HNO_2. We hesitate, however, to introduce additional species and further adjustable parameters into the model without more experimental information about the reactions involved. Nevertheless, the results obtained even with this simplified model make the Fe(II)–HNO_3 reaction one of the best understood of the known bistable systems.

Whether this system, like several earlier bistable reactions, can be modified so as to produce oscillation in a CSTR is still open to question. Our initial attempts have not met with success. The cross-shaped phase diagram approach[4b] suggests that we search for a feedback reaction which affects the stabilities of the two bistable branches differently. However, the theory also requires that the feedback reaction be much slower than the relaxation to the steady states of the Fe^{2+}–HNO_3 subsystem. Unfortunately, this relaxation is relatively slow compared with that of the bistable oxyhalogen systems which lead to oscillation,[6,7] and we have not yet been able to find a feedback species which acts sufficiently slowly to modify the effective concentration of one of the reactants.

A possible solution to this problem may lie in complexing the iron with various ligands in order to accelerate reactions P1–P3. Also, reaction P4 may have a damping effect on the system by removing NO which is a key species in the autocatalysis.[8] If a ferrous complex (or a different species) can be found which still reacts autocatalytically, but does not bind NO as strongly, the relaxation process may be speeded and the prospects for oscillation enhanced. We note that a number of nitric acid oxidations, including those of arsenite,[19] thiocyanate,[20] and hydroxylamine,[21] have been reported to be autocatalytic. Investigation of these possibilities is under way.

Acknowledgment. This work was supported by Grant No. CHE-7905911 from the National Science Foundation. We thank Patrick De Kepper and Kenneth Kustin for a number of thoughtful suggestions.

Registry No. Fe, 7439-89-6; nitric acid, 7697-37-2.

(18) Epstein, I. R.; Kustin, K.; Simoyi, R. M. *J. Am. Chem. Soc.* **1982**, *104*, 712–717.

(19) Abel, E.; Schmid, H.; Weiss, J. *Z. Phys. Chem. Abt. A* **1930**, *147*, 69–86.

(20) (a) Stedman, G.; Whincup, P. A. E. *J. Chem. Soc. A* **1969**, 1145–1148. (b) Hughes, M. N.; Phillips, E. D.; Stedman, G.; Whincup, P. A. E. *J. Chem. Soc. A* **1969**, 1148–1151.

(21) Stedman, G. *Adv. Inorg. Chem. Radiochem.* **1979**, *22*, 113–170.

X-ray Photoelectron Spectroscopic Study of the Enol–Enethiol Tautomerism of Thioacetylacetone and Related β-Thioxoketones[1]

Flemming S. Jørgensen,*[2a] R. S. Brown,[2b] Lars Carlsen,[2c] and Fritz Duus[2d]

Contribution from the Department of General and Organic Chemistry, The H. C. Ørsted Institute, University of Copenhagen, DK-2100 Copenhagen Ø, Denmark, the Department of Chemistry, University of Alberta, Edmonton, Alberta T6G 2G2, Canada, the Chemistry Department, Risø National Laboratory, DK-4000 Roskilde, Denmark, and the Institute of Life Sciences and Chemistry, Roskilde University, DK-4000 Roskilde, Denmark. *Received October 15, 1981*

Abstract: X-ray photoelectron spectroscopy has been used to record the O_{1s} and S_{2p} ionization spectra of thioacetylacetone, 2-acetylcyclohexanethione, 2-thioacetylcyclohexanone, the *S*-methyl derivative of thioacetylacetone, and propyl 3-mercaptocrotonate in the gas phase. It is shown that both the enol and the enethiol tautomers of the β-thioxoketones can be detected, and the enol/enethiol ratios for thioacetylacetone, 2-acetylcyclohexanethione, and 2-thioacetylcyclohexanone were determined to be 61:39, 30:70, and 80:20, respectively, based on the intensities of the oxygen ionizations. The conclusions derived from the sulfur region support the above, although they are less clear due to sulfur spin–orbit splitting. The enol/enethiol ratios obtained in the gas phase by XPS are compared with data from other methods, showing good agreement between results obtained in the gas phase and in solution. The binding energy (BE) shifts of the O_{1s} and S_{2p} orbitals have been discussed and suggest that geometrical factors affect the strength of the intramolecular hydrogen bond.

Introduction

In recent years much effort has been devoted to study the keto–enol tautomerism in β-diketones **1**.[3] Replacement of one

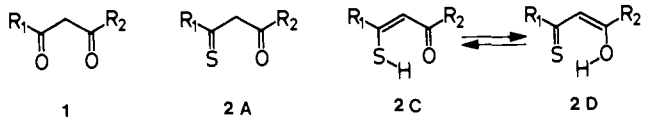

1 2A 2C 2D

of the oxygen atoms by a sulfur atom leads to β-thioxoketones **2**.[4,5] In contrast to the oxygen analogues the β-thioxoketones exist principally as rapidly interconverting tautomeric forms, the enol **2D** and enethiol **2C** forms, whereas the thioxoketone structure has never been observed.[6-12]

(1) β-Thioxoketones. Part 8. For part 7, see ref 6.

(2) (a) University of Copenhagen; (b) University of Alberta; (c) Risø National Laboratory; (d) Roskilde University.

(3) S. Forsén and M. Nilsson in "The Chemistry of the Carbonyl Group", Vol. 2, J. Zabicky, Ed., Interscience, London, 1970, Chapter 3.

(4) The β-thioxoketones are named as such for simplicity, regardless of which tautomer is present. The notation of the tautomeric forms is consistent with that in previous parts.

(5) For a recent review see F. Duus (D. N. Jones, Vol. Ed.) in "Comprehensive Organic Chemistry", Vol. 3, D. H. R. Barton and W. D. Ollis, Eds., Pergamon Press, Oxford, 1979, Chapter 11.22.

(6) F. S. Jørgensen, L. Carlsen, and F. Duus, *J. Am. Chem. Soc.*, **103**, 1350 (1981).

(7) L. Carlsen and F. Duus, *J. Am. Chem. Soc.*, **100**, 281 (1978).

(8) L. Carlsen and F. Duus, *J. Chem. Soc., Perkin Trans 2*, 1768 (1980).

(9) L. Carlsen and F. Duus, *J. Chem. Soc., Perkin Trans 2*, 1532 (1979).

(10) L. Carlsen and F. Duus, *J. Chem. Soc., Perkin Trans 2*, 1080 (1980).

(11) F. Duus and J. W. Anthonsen, *Acta Chem. Scand. Ser., B*, **31**, 40 (1977).

0002-7863/82/1504-5922$01.25/0 © 1982 American Chemical Society